clude its chance of failure once it has been installed in the vehicle. This approach is attractive not only because of its technical soundness, but also because of the economically responsible manner in which it can be accomplished.

With respect to the cost of testing, in the erection to launch cycle of 19 vehicles taken in consecutive order from two programs, there were 3693 airborne and ground system components replaced that resulted in 17 successful flights and two catastrophic failures.

Add to the 3693 component replacements the irrefutable fact that they all occurred at the most expensive end of the development to launch sequence, as illustrated in Fig. 2,[1] and you have the premise for the basic conclusion which resulted from this investigation.

Over the past several years, some form of a successful Combined Systems Test or Simulated Flight has attained the status of being almost synonymous with successful flight. In fact, every vehicle that flew successfully was preceded by a successful Combined Systems Test. It is also a fact that every vehicle that failed was preceded by a successful Combined Systems Test.

This type of test is effective for examining the status of electrical components in a nonflight environment and for determining the integrity of system interfaces, but it cannot detect incipient, dynamic failure modes, and it has not proved useful in detecting or preventing the basic cause of flight failure.

An analysis of all of the flight failures included revealed that 90% were mechanical, electro-mechanical, or structural. Of these, some 48% occurred in components involving no moving parts. The remaining 52% involved mechanical or electro-mechanical components that utilized moving parts to perform their function. This ratio points out that the seemingly "simple" mechanical and structural components' relevance to flight failure is equally as significant as the more complicated components with moving parts.

From the flight data, it was determined that mechanical failures usually occur on parts under stress or operating conditions that take place only during the dynamics of flight, and therefore cannot be tested on the assembled static vehicle. Again, the same conclusion is supported. Adequate preflight testing on most mechanical or electro-mechanical components can only be conducted during design development, qualification, and acceptance testing.

Throughout the research that went into the preparation of this study, we were also frequently exposed to discussions and reports dealing with circumstances that ostensibly prohibit the conduct of adequate testing. There were indications that this impossible-to-test situation is sometimes underwritten by economic restraints, by compression of time, by design limitations, or by the very nature of the devices to be tested.

We noted, however, that subsequent to flight failure, no component or system, even those previously labeled "impossible-to-test," escaped exhaustive scrutiny. All systems and all components were suddenly "testable." We found that no impossible-to-test cases existed when: 1) all development failures were treated as though they were flight failures and received the same corrective action that would have been afforded a flight failed component, or 2) testing was done to the flight environment before the failure instead of after, by applying the same foresight to the development and acceptance tests before flights as was done after flight failure.

The economic gains of designing for test are yet to be fully recognized. In the large launch vehicle systems studies, we found many very real limitations still exist in performing checkout operations. Although electrical checkout, in more cases, has been automated to a sophisticated level, there are still mechanical operations which are reminiscent of the white scarf and goggles era. Connectors must be mated and demated; simulators and test tools must be installed and removed; personnel access must be made to various areas of the vehicle with no reasonable provision for such access; facility requirements of a massive and complicated nature result from a reluctance to accommodate vehicle design with simple preparation and checkout provisions. This study disclosed that, conservatively, 30% of launch site test crew effort was expended exclusively on maintenance of facility and ground equipment which had only a secondary relationship to launch vehicle activity.

In our investigations, we found that the test sequence which a component follows from its physical inception to flight is essentially the same for all missile and space systems.

Moreover, elements of development, qualifications, acceptance, subsystem, and then flight simulation are in logical order. The illogic of this scheme stems from a fundamental lack of definition of what each of these basic elements is expected to accomplish; in short, missile test and launch organizations have no clearly defined philosophy behind testing.

The cost of detecting and correcting defects rises sharply as the point of detection moves closer to flight, with the ultimate price being paid when detection occurs during flight itself. On the other hand, there is little understanding, and no clear policy, that launch operations testing can only be economically useful when it is involved in determining system interface integrity and not in weeding out defective components that should have been eliminated prior to the vehicle's arrival at the test range.

The large complements of personnel necessary today to operate and maintain launch operations can be substantially reduced if the test engineer will bring his experience to bear on the design concept. The fundamental responsibility for the serious development of these solutions rests with the test organization itself—and it has, literally, done little to solve them. The course this nation's space effort follows over the next several years may well be affected by the insight, the energy and the shrewdness which launch operations organizations apply to maturing their role in the aerospace community.

Reference

[1] Cornell, C. E., "Minimizing Human Errors," *Space Aeronautics Magazine*, March 1968, pp. 72–81.

Effect of Specific Heat Ratio on Surface Pressure Coefficient for Lifting Cones

D. J. Jones*
National Aeronautical Establishment, Ottawa, Canada

Nomenclature

C_p	=	surface pressure coefficient, $2(p - p_\infty)/\gamma p_\infty M^2$
$C_p{}^A, C_p{}^B$	=	values of C_p for $\gamma = 7/5$ and $\gamma = 5/3$
$C_p{}^R$	=	value of C_p at $\alpha = 0$ with $\gamma = 7/5$ for the same M, θ_c combination for which $C_p{}^A - C_p{}^B$ is being examined; i.e., $C_p{}^R \equiv (C_p{}^A)_{\alpha=0}$
K	=	hypersonic similarity parameter, $K \equiv M \sin\theta_c$
M	=	freestream Mach number
p, p_∞	=	surface pressure and freestream pressure
γ	=	ratio of specific heats
θ_c	=	cone half-angle
α	=	angle of incidence
ϕ	=	circumferential angle; $\phi = 0$ is the windward plane of symmetry

Received March 4, 1970; revision received June 8, 1970.
* Mathematician. Member AIAA.

THE author has recently computed flowfields about yawed conical bodies in supersonic streams. The method is given in Ref. 1, and results for circular cones with half-angle θ_c ranging from 5° to 40°, Mach numbers from 1.5 to 20, and relative incidences α/θ_c up to $\sim$ 1.0 are given in Ref. 2, all for γ = constant = 1.4. In the present Note it is illustrated that over a large range of M, θ_c, and α/θ_c the values for C_p with $\gamma = 5/3$ differ by only $\sim$2% on the average from the values obtained with $\gamma = 7/5$.

Approximate Analytical Formulae for C_p

Two types of approximate solution are available: slender-body theory applicable to small changes in quantities, and the solution based on hypersonic conditions. Slender-body theory[3] is based on the assumption that quantities change by only a small amount both across the shock wave and within the flowfield, hence it is applicable to conditions of sufficiently small K. Surface pressure predicted by slender body theory shows excellent agreement with the exact solutions for small K for all values of α/θ_c considered.[2] Since C_p has no dependence on γ in this theory, it is to be expected that C_p is almost constant for values of K sufficiently small. This prediction turns out to be true of the numerical solutions as will be seen later.

Several approximate formulas are available for C_p under hypersonic conditions. Cheng's[4] formulas are accurate for large M and to second order in α. Lees' fairly complicated pressure formula[5] is not accurate when K is small. Rasmussen[6] derived a simple approximate pressure formula for hypersonic flow past an unyawed cone using hypersonic small disturbance theory and showed that the formula, for θ_c's of 5° and 30°, is quite accurate when $K > 1$. In this Note Rasmussen's pressure formula is considered so as to give some indication of the pressure variation with γ. Although this formula is applicable only to zero incidence, this is sufficient for our purpose, since incidence variation can be accounted for by tangent cone approximations.[7] The C_p formula given by Rasmussen is

$$\frac{C_p}{\sin^2\theta_c} = 1 + \frac{(\gamma+1)K^2+2}{(\gamma-1)K^2+2}\log\left(\frac{\gamma+1}{2}+\frac{1}{K^2}\right) \quad (1)$$

Using this formula it is found that $(C_p{}^A - C_p{}^B)/C_p{}^A$ is small, increasing from 1.5% at $K = 1$ to 2.6% at $K = \infty$ (see Fig. 1). With this evidence of little difference in C_p for the two values of γ being considered, it appears to be worthwhile to examine the differences for various M, θ_c combinations, as follows.

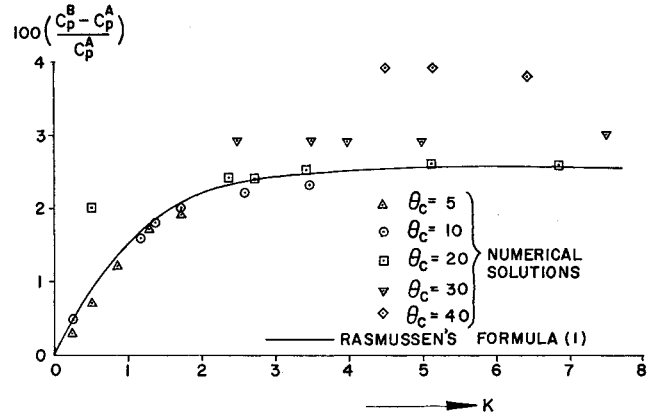

Fig. 1 Relative pressure differences at zero incidence vs K.

Numerical Solutions

Numerical solutions are obtained by the method described in Ref. 1. In this Note we examine $(C_p{}^B - C_p{}^A)$ relative to $C_p{}^R$, which is taken to be $C_p{}^A$ at $\alpha = 0°$ for the same M, θ_c combination. Table 1 lists, for all circumferential angles ϕ, some typical values of $C_p{}^A$, $C_p{}^B$ and the relative differences as just defined. It can be seen that the difference is practically zero for the results where slender-body theory would apply and appears to be in agreement with what is expected from Rasmussen's analytical formula (except for the 40° cone, where the errors are a little higher than those predicted by Rasmussen; see Fig. 1). On examining the relative differences for conditions between slender-body and hypersonic it is observed that the maximum error appears to be about 4% (see the last line in Table 1). It is also seen from Table 1 that, at incidence, the relative differences for a given M, θ_c combination are, in most cases, characterized by the difference at zero incidence for the same Mach number and cone angle combination.

References

[1] Jones, D. J., "Numerical Solutions of the Flow Field for Conical Bodies in a Supersonic Stream," Rept. LR-507, 1968, National Research Council of Canada.

Table 1 C_p values and relative differences; upper line $C_p{}^B$, middle line $C_p{}^A$, lower line 100 $[(C_p{}^B - C_p{}^A)/C_p{}^R]$

M	θ_c	K	$\alpha/\theta_c = 0$	α/θ_c	$\phi = 0$	22.5	45	67.5	90	112.5	135	157.5	180
3	5	0.26	0.0283	0.5	0.0453	0.0433	0.0379	0.0309	0.0243	0.0195	0.0170	0.0162	0.0160
			0.0282		0.0452	0.0432	0.0379	0.0309	0.0242	0.0195	0.0170	0.0161	0.0160
			0.3		0.3	0.3	0.2	0.2	0.2	0.2	0.2	0.2	0.2
7	10	1.21	0.0710	0.6	0.1602	0.1512	0.1272	0.0956	0.0648	0.0408	0.0264	0.0209	0.0199
			0.0699		0.1590	0.1501	0.1265	0.0954	0.0648	0.0408	0.0262	0.0204	0.0193
			1.6		1.8	1.6	1.0	0.4	−0.1	−0.1	0.3	0.7	0.9
				1.2	0.2847	0.2597	0.1943	0.1259	0.0549	0.0169	−0.0110	−0.0085	0.0035
					0.2842	0.2597	0.1950	0.1273	0.0572	0.0182	−0.0094	−0.0089	0.0024
					0.7	0	−0.9	−2.0	−3.2	−2.0	−2.3	−0.6	1.7
7	20	2.39	0.2591	0.4	0.4645	0.4446	0.3907	0.3176	0.2429	0.1806	0.1381	0.1157	0.1092
			0.2531		0.4582	0.4385	0.3851	0.3129	0.2391	0.1773	0.1347	0.1119	0.1050
			2.4		2.5	2.4	2.2	1.9	1.5	1.3	1.3	1.5	1.6
				0.8	0.7071	0.6573	0.5270	0.3629	0.2138	0.1068	0.0455	0.0255	0.0274
					0.7027	0.6531	0.5235	0.3608	0.2128	0.1073	0.0457	0.0236	0.0245
					1.7	1.7	1.4	0.8	0.4	−0.2	−0.1	0.7	1.2
8	30	4.0	0.5468	0.6	1.1396	1.0732	0.8969	0.6677	0.4469	0.2758	0.1681	0.1237	0.1186
			0.5313		1.1265	1.0604	0.8851	0.6574	0.4387	0.2695	0.1620	0.1170	0.1093
			2.9		2.5	2.4	2.2	1.9	1.6	1.2	1.1	1.3	1.7
7	40	4.5	0.9155	0.2	1.1942	1.1678	1.0948	0.9919	0.8804	0.7801	0.7048	0.6600	0.6454
			0.8809		1.1568	1.1310	1.0597	0.9590	0.8495	0.7503	0.6748	0.6289	0.6137
			3.9		4.2	4.2	4.0	3.7	3.5	3.4	3.4	3.5	3.6

[2] Jones, D. J., "Tables of Inviscid Supersonic Flow About Circular Cones at Incidence, $\gamma = 1.4$," AGARDograph No. 137, Nov. 1969.
[3] Sears, W. R., *"General Theory of High Speed Aerodynamics,* Vol. 6, Oxford University Press, 1955, pp. 238–239.
[4] Cheng, H. K., "Hypersonic Shock Layer Theory of a Yawed Cone and Other Three Dimensional Bodies," *Journal of Fluid Mechanics,* Vol. 12, No. 2, 1962, p. 169.
[5] Lees, L., "Note on the Hypersonic Similarity Law for an Unyawed Cone," *Journal of the Aeronautical Sciences,* Vol. 18, 1951, pp. 700–702.
[6] Rasmussen, M. L., "On Hypersonic Flow Past an Unyawed Cone," *AIAA Journal,* Vol. 5, No. 8, Aug. 1967, pp. 1495–1497.
[7] Chernyi, G. G., *Introduction to Hypersonic Flow,* Academic Press, New York, 1961, pp. 113–120.

Analysis of Jimsphere Wind Profiles Viewed in the Flight Time Domain of a Saturn Vehicle

S. I. ADELFANG*
Lockheed-California Company, Burbank, Calif.

NINE hundred Jimsphere wind profiles obtained over Cape Kennedy, Fla., between November 1964 and May 1967 were used for an analysis of horizontal wind speeds viewed by a Saturn vehicle in an AS-504 trajectory. Each profile was evaluated at $\frac{1}{6}$-sec intervals of AS-504 vehicle flight time and high-pass-filtered to remove low-frequency fluctuations that would not involve significant control and structural responses in the vehicle. This paper describes the distribution of gusts, gust variance, and spectrum densities observed in these profiles.

Gust Profile Definition

Vehicle response characteristics are usually defined in terms of temporal frequency f (cps) rather than spatial frequency K (cpm). As a vehicle ascends with vertical velocity $v(t)$ through the atmosphere, wind fluctuations at spatial frequency K are seen by the vehicle at frequency f given by

$$f = Kv(t) \tag{1}$$

Thus, for example, the fluctuations in the wind profile at $K = 2.74.10^{-3}$ (cpm) as seen by a Saturn vehicle increase from $f = 0.534$ cps at 4 km ($v = 195$m/sec) to $f = 1.00$ cps at 12 km ($v = 365$m/sec). Since the first bending mode frequency of a Saturn 5 vehicle is approximately 1 cps, the fluctuations at $K = 2.74.10^{-3}$ cpm are more important at 12 km than at 4 km. Innumerable spatial frequencies exist for a particular critical value of temporal vehicle response frequency; therefore, it is necessary to transform the spatial fluctuations of wind profiles to temporal fluctuations as seen by the vehicle.

The general procedure suggested in Ref. 1 for deriving gust profiles is used for this study. Jimsphere wind profiles are transformed to vehicle time coordinates by evaluating them at altitudes Z (km) corresponding to the time, t (sec), from launch at intervals of time Δt (sec), according to the least-squares quadratic fit to the Saturn AS-504 trajectory given by Jacobs[2]:

$$Z = 2.98416 - 0.14889t + 0.00330t^2 \tag{2}$$

Z calculated from Eq. (2) deviates less than 1.7% from the AS-504 trajectory for the time interval from 50 to 95 sec ($Z = 3.855$ to 18.530 km). The time interval Δt was chosen small enough to include all Jimsphere data up to 17.2 km. Assuming that a Jimsphere profile contains independent estimates of wind over 75 m altitude intervals, the time interval Δt (sec) between independent wind estimates as seen by a vehicle is $75/v(t)$; at 17.2 km, for Saturn AS-504, $v(t) = 450$ m/sec, hence $\Delta t = \frac{1}{6}$ sec.

The transformed wind profile is an approximation of the profile "seen" by the vehicle; the accuracy of the approximation for space vehicle studies is not yet known and may only be determined when the statistics of vehicle responses derived from simulated flights through Jimsphere wind profiles are compared to the same statistics derived from wind profile data obtained from sensors which traverse the atmosphere in space-time coordinates that are similar to those of space vehicles.

The fluctuations of interest, which will be referred to as gusts, are characterized by their influence on space vehicle control and structural excitation frequency modes. For a Saturn vehicle significant response to wind fluctuations occur at the control frequency (~0.2 cps) and at the first and second bending mode frequencies (~1.2 cps). Wind profiles which have fluctuations at frequencies ≥0.2 cps are defined as gust profiles. Gust profiles were calculated by application of a 33 weight digital high-pass filter which has a transfer function of the form

$$H(f) = 1 - \exp[-39.2f/f_s]^2 \tag{3}$$

Table 1 Symmetrical 33 weight digital high-pass filter with transfer function given by Eq. (4); $\Delta t = \frac{1}{6}$ sec

Time	Numerical weights
t	0.951844
$-\Delta t + \Delta t$	−0.047848
$-2\Delta t + 2\Delta t$	−0.046936
$-3\Delta t$, etc.	−0.045453
...	−0.043457
...	−0.041013
...	−0.038222
...	−0.035162
...	−0.031935
...	−0.028634
...	−0.025346
...	−0.022151
...	−0.019110
...	−0.016288
...	−0.013689
...	−0.011364
$-16\Delta t$, $+16\Delta t$	−0.009314

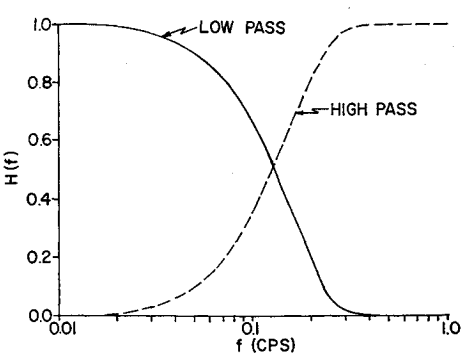

Fig. 1 Transfer functions of Alfriend exponential low-pass and high-pass filters for a sampling frequency of 6 sec^{-1}.

Received May 4, 1970; revision received June 19, 1970. The author expresses his appreciation to the Aerospace Environment Division, Aero-Astrodynamics Laboratory, NASA, Huntsville, Ala. for their support of this research under Contract NAS 8-30165.

* Research Scientist.